

Lifetime measurement of the first excited 2^+ state in ^{108}Te

T. Bäck,^{1,*} C. Qi,¹ F. Ghazi Moradi,¹ B. Cederwall,¹ A. Johnson,¹ R. Liotta,¹ R. Wyss,¹ H. Al-Azri,² D. Bloor,² T. Brock,² R. Wadsworth,² T. Grahn,³ P. T. Greenlees,³ K. Hauschild,^{3,†} A. Herzan,³ U. Jacobsson,³ P. M. Jones,³ R. Julin,³ S. Juutinen,³ S. Ketelhut,³ M. Leino,³ A. Lopez-Martens,^{3,†} P. Nieminen,³ P. Peura,³ P. Rahkila,³ S. Rinta-Antila,³ P. Ruotsalainen,³ M. Sandzelius,³ J. Sarén,³ C. Scholey,³ J. Sorri,³ J. Uusitalo,³ S. Go,⁴ E. Ideguchi,⁴ D. M. Cullen,⁵ M. G. Procter,⁵ T. Braunroth,⁶ A. Dewald,⁶ C. Fransen,⁶ M. Hackstein,⁶ J. Litzinger,⁶ and W. Rother⁶

¹Royal Institute of Technology, SE-10691 Stockholm, Sweden

²Department of Physics, University of York, YO10 5DD York, United Kingdom

³Department of Physics, University of Jyväskylä, FIN-40014 Jyväskylä, Finland

⁴CNS, University of Tokyo, Wako-shi, Saitama, Japan

⁵School of Physics and Astronomy, Schuster Laboratory, University of Manchester, Manchester M13 9PL, United Kingdom

⁶Institut für Kernphysik, Universität zu Köln, Zùlpicher Straße 77, D-50937 Köln, Germany

(Received 31 May 2011; published 31 October 2011)

The lifetime of the first excited 2^+ state in the neutron deficient nuclide ^{108}Te has been measured for the first time, using a combined recoil decay tagging and recoil distance Doppler shift technique. The deduced reduced transition probability is $B(E2; 0_{\text{g.s.}}^+ \rightarrow 2^+) = 0.39_{-0.04}^{+0.05} e^2\text{b}^2$. Compared to previous experimental data on neutron deficient tellurium isotopes, the new data point constitutes a large step (six neutrons) toward the $N = 50$ shell closure. In contrast to what has earlier been reported for the light tin isotopes, our result for tellurium does not show any enhanced transition probability with respect to the theoretical predictions and the tellurium systematics including the new data is successfully reproduced by state-of-the-art shell model calculations.

DOI: [10.1103/PhysRevC.84.041306](https://doi.org/10.1103/PhysRevC.84.041306)

PACS number(s): 21.10.Tg, 21.60.Cs, 27.60.+j

The structure of atomic nuclei near the presumed doubly magic nucleus ^{100}Sn has been at the focus of numerous experimental and theoretical studies. As we approach the $N = Z$ line and the closed shells at ^{100}Sn , the shell structure is of fundamental interest for our understanding of the nature of the nucleon-nucleon interaction inside the nucleus. The experimental efforts to extend the *energy* spectroscopy in the region is ongoing, and continues to give new information. But in order to probe the models further, and to be able to explain new phenomena complementary measurements of other quantities, such as nuclear masses and transition probabilities, are just as important. In the neutron deficient even-mass Sn isotopes a series of experiments using Coulomb excitation have revealed $B(E2; 0_{\text{g.s.}}^+ \rightarrow 2^+)$ systematics that could not easily be explained by theoretical calculations [1–4]. Neither the intuitive scheme of generalized seniority [5], nor standard large-scale shell model calculations could so far reproduce the experimental data. As we decrease the number of neutrons from midshell and approach the $N = 50$ shell gap, the reduced transition probabilities are expected to drop, according to such model predictions. However, the experimental results reported for the neutron deficient Sn isotopes, albeit with large uncertainties, lie more or less constant around the mid-shell values. This unusual feature has been discussed in terms of a “weakening” of the $N = Z = 50$ shell closures [4]. As the most relevant shell-model orbitals above the Fermi surface are the same for the $_{50}\text{Sn}$ and $_{52}\text{Te}$ isotopes, i.e., $g_{7/2}$, $d_{5/2}$, $d_{3/2}$, $s_{1/2}$, $h_{11/2}$, we would expect that $B(E2)$ data

for tellurium isotopes can give valuable clues for solving this apparent conundrum. In this region of the nuclide chart neutrons and protons occupy the same orbitals, leading to enhanced neutron-proton (np) interactions. Therefore, if the $N = Z = 50$ shell-gap energy would be reduced, as discussed in Ref. [4], we would expect, additionally, a significant enhancement of the transition probabilities also in light Te isotopes.

In this work we present a lifetime measurement of the first excited 2^+ state in the neutron deficient tellurium isotope ^{108}Te . The $B(E2)$ data for neutron deficient tellurium isotopes is quite scarce. Before the present experiment, no $B(E2)$ values for tellurium isotopes lighter than ^{114}Te have been reported. The big “leap” toward $N = Z$ in this region was only made possible by the unique combination of a differential plunger technique and the recoil-decay-tagging method, see also Ref. [6].

The experiment was performed at the Accelerator Laboratory of the Department of Physics at the University of Jyväskylä (JYFL), Finland. A beam of ^{58}Ni ions was accelerated by the JYFL K130 cyclotron to an energy of 245 MeV. The Ni ions bombarded a production target of ^{54}Fe (areal density 1 mg/cm², 99.8% isotopic enrichment) at the center of the JUROGAM II γ -ray detector array, combining escape-suppressed germanium detectors of two types from the former Euroball array [7]: 15 Phase-I type detectors and 24 segmented clovers [8]. Gamma rays emitted from the recoiling fusion-evaporation products were detected by the JUROGAM II detectors. The recoiling ^{108}Te nuclei were subsequently transported through the gas-filled RITU recoil separator [9], and implanted in the pixelated double-sided silicon strip detector of the focal plane detector system GREAT [10]. With the recoil decay tagging (RDT) technique [11,12] the unique ground state α decay energy of ^{108}Te enabled a clean selection

*Corresponding author: back@nuclear.kth.se

†Present address: CSNSM, IN2P3-CNRS et Université Paris Sud, Paris, France.

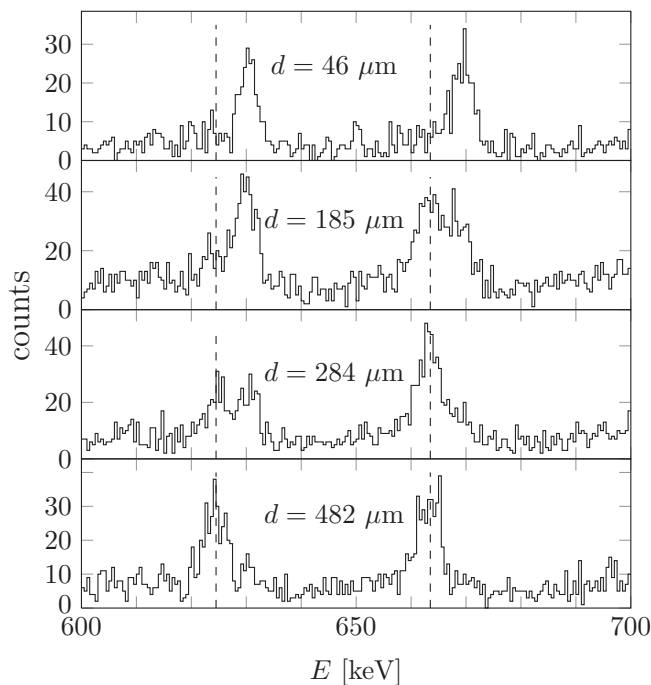


FIG. 1. Gamma-ray energy spectra from ten JUROGAM II detectors at the angle $\theta = 134^\circ$ showing the $2^+ \rightarrow 0^+$ and $4^+ \rightarrow 2^+$ ^{108}Te transitions at 625 keV and 664 keV, respectively (dashed lines). As the target-to-degrader distance, d , increases, the peaks shift from the positions corresponding to the lower velocity *after* the degrader to the position corresponding to the higher velocity *before* the degrader. The spectra shown are Doppler corrected for this higher velocity.

of γ rays belonging to the $^{54}\text{Fe}(^{58}\text{Ni}, 2p2n)^{108}\text{Te}$ reaction channel. A maximum correlation time of 6 s (approximately three half-lives for the ground state of ^{108}Te) was used between the recoil implantation and the subsequent α decay. In order to measure the lifetimes of excited states in ^{108}Te , the RDT setup was combined with a recoil distance Doppler shift technique, using the Köln differential plunger [13]. In this device a degrader foil (natural Mg, 1 mg/cm²) was positioned at a number of controlled distances from the target foil during the experiment. In order to avoid fluctuations in the target-to-degrader foil distance, the beam current was limited to 1 particle nA. The detector data were collected through the Total Data Readout system [14] by recording time-stamped events from the large number of detector channels around the target as well as around the RITU focal plane. The data were sorted off-line using the GRAIN software package [15] and analyzed using the RADWARE software package [16]. The lifetime, τ , was extracted using the well established differential decay curve method (DDCM) [17].

For eight different plunger distances, using Phase-I Ge-detectors at the angle $\theta = 134^\circ$, the quantities I_s and I_d (intensity of the shifted and degraded component, respectively) were extracted from gamma-ray energy spectra, some of which are shown in Fig. 1. The spectra, tagged by the ^{108}Te α decay, illustrate how the Doppler shifts depend on the target-to-degrader distance as a consequence of the finite

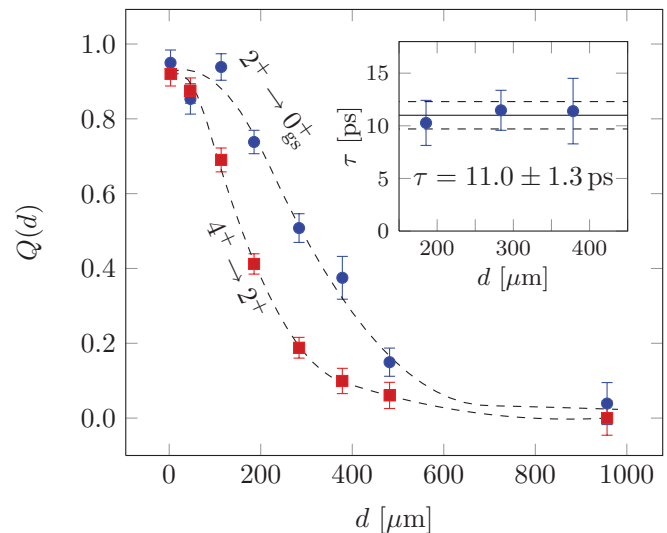


FIG. 2. (Color online) Relative intensities, $Q(d)$, for the $2^+ \rightarrow 0^+_{\text{g.s.}}$ (blue circles) and $4^+ \rightarrow 2^+$ (red squares) γ -ray transitions in ^{108}Te . Inset: The lifetime is deduced according to Ref. [17] for three distances (185 μm , 284 μm , 378 μm) in the region where the slope of the $2^+ \rightarrow 0^+_{\text{g.s.}}$ curve is well defined. The error bars reflect statistical uncertainties of Q . The uncertainty in d is below 1 μm for all data points, except at 957(19) μm .

lifetimes of the excited states. Following Ref. [17], the quantity $Q = I_d/(I_s + I_d)$ is plotted as a function of the plunger distance, d , in Fig. 2 for the two transitions $4^+ \rightarrow 2^+$ and $2^+ \rightarrow 0^+_{\text{g.s.}}$. The software APATHIE [18] was used for extracting the derivative (with uncertainties) of $Q(d)$. The figure inset shows deduced lifetime values for three distances, d . The constant (within errors) value as a function of d indicates that the simple assumptions about the feeding pattern, see below, are valid. With a measured velocity (between target and degrader) of $v/c = 0.0431(4)$, the weighted average lifetime value for the 2^+ state was $\tau = 11.0 \pm 1.3$ ps, corresponding to a $B(E2; 0^+_{\text{g.s.}} \rightarrow 2^+)$ value of $0.39^{+0.05}_{-0.04} e^2 b^2$.

Several experimental aspects are of importance and should be handled with care when determining $B(E2)$ values by lifetime measurement of excited states in nuclei. One crucial detail is the pattern of intensity feeding into the excited levels of interest [17]. The time structure of all feeding branches to an excited state will affect the distribution of decay times from that state, and therefore also the position-of-decay in a plunger experiment. Both the observed feeding and the unobserved feeding (realized from missing intensity) will then affect the measurement. This problem can be handled in different ways, and a common technique is to use energy gates to *select* one feeding branch. However, when the reaction channel is too weakly populated, as in the present case, such coincidence techniques cannot be used. Fortunately, the case of the 2^+ state in ^{108}Te is quite favored, since the intensities of the $2^+ \rightarrow 0^+_{\text{g.s.}}$ and the $4^+ \rightarrow 2^+$ transitions are the same, within the statistical uncertainties, in the present experiment. The level scheme and feeding patterns of ^{108}Te are well known from earlier experiments [19,20]. The lack of side feeding to the 2^+ state is related to the nonobservation of the 3^- state in

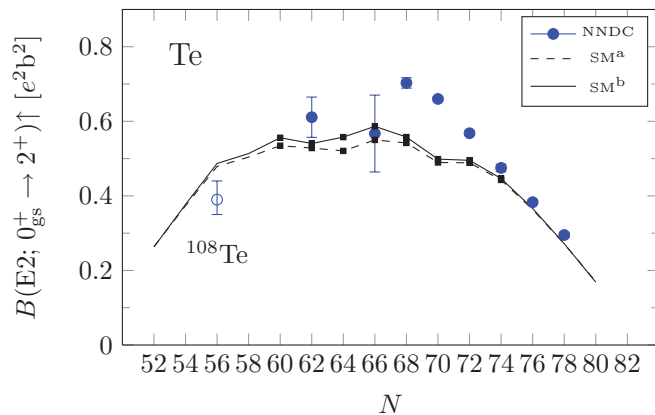


FIG. 3. (Color online) Upper panel: Experimental $B(E2)$ values for Te isotopes (solid circles), together with the new $B(E2)$ data point for ^{108}Te (open circle). The data are compared to the shell model calculation with ε_{sp} values according to Ref. [1] (SM^a , dashed line) and with the $d_{5/2}$, $g_{7/2}$ orbitals inverted, see text (SM^b , solid line). The effective charges used were $e_{\text{eff}}^v = 0.8e$, $e_{\text{eff}}^\pi = 1.5e$. For the midshell (small solid squares), the model space ($g_{7/2}$, d , s , $h_{11/2}$) was limited, allowing excitations of up to four neutrons above the Fermi level in the $h_{11/2}$ subshell. This leads to the underestimation in the model predictions visible around midshell.

the negative parity band, as was discussed by Lane *et al.* [20]. In this particular case, it is therefore sufficient to record the decay time pattern of these two transitions to determine the lifetime of the 2^+ state and from that deduce the $B(E2; 0_{\text{g.s.}}^+ \rightarrow 2^+)$ value. The fact that the lifetime value is constant, within statistical errors, for three separate target-degrader distances, see Fig. 2, gives additional rigidity to the measurement. The DDCM method used in the present analysis allowed us to measure the half-life of ^{108}Te without the need for any normalization to values of other nuclides. We also point out here that the DDCM method is insensitive to the *absolute* plunger distance, which significantly reduces the risk of introducing systematic errors.

The nuclear shell model has a long and successful track record in explaining nuclear structure phenomena in the vicinity of closed shells. As in other regions of the nuclide chart, its success to describe nuclear properties near ^{100}Sn , depends on detailed knowledge of the active single particle states. Above the $N, Z = 50$ shell closure the situation is complex and even the relative ordering of the $g_{7/2}$ and $d_{5/2}$ orbitals has been actively debated [21–23]. Here, a substantial influence from several orbitals is present, and already for nuclides with a small number of nucleons above the shell gap a large shell model space is required, making the calculations very demanding even on present day high-performance computers. The difficulties to model the nuclei in this region are further exacerbated by the limited experimental data in this far-from-stability region (e.g., the lack of known masses and single particle energies).

In the present study, we have compared the experimental data on reduced transition probabilities for Te isotopes with the results of new large-scale shell model calculations involving the neutron and proton orbitals $g_{7/2}$, $d_{5/2}$, $d_{3/2}$, $s_{1/2}$, and $h_{11/2}$. In the calculation, we use the CD-Bonn interaction [24],

renormalized by using the perturbation approach according to Ref. [25]. The calculations were performed with two sets of single particle energies, ε_{sp} . In the first set, the values for ε_{sp} were taken from Ref. [1]. In the second set, the new result in Ref. [21] was taken into account by setting $\varepsilon_{sp}(g_{7/2}) = 0$ and $\varepsilon_{sp}(d_{5/2}) = 172$ keV. In the upper panel of Fig. 3 the resulting shell model predictions of $B(E2; 0_{\text{g.s.}}^+ \rightarrow 2^+)$ in tellurium isotopes are compared to experimental data. The effective charges in this region are not well known, see, e.g., the discussion in Ref. [26]. With $e_{\text{eff}}^v = 0.8$ and $e_{\text{eff}}^\pi = 1.5$ the calculated values in the model space $g_{7/2}$, d , s , $h_{11/2}$ reproduce the experimental $B(E2)$ values quite well. The reduced values of the model predictions around midshell compared with the experimental data is an expected effect due to the limitation in occupation of the the $h_{11/2}$ orbital allowing excitations of up to four neutrons above the Fermi level (our current computing limit). Below $N = 60$ and above $N = 74$ this limitation is removed. The model prediction agrees rather well with the new data point for ^{108}Te . To our knowledge, large-scale shell model calculations of $B(E2)$ values across the chain of even-mass Te isotopes have not been reported prior to this work. The calculations are challenging, even with large-scale computer clusters, due to the large matrix dimensions involved (10^{10} at midshell, compared to 10^8 for Sn).

The recent measurements of reduced transition probabilities in neutron deficient Sn isotopes have revealed values about 30% above the shell model predictions presented in Refs. [1–4]. Not even when taking into account the $g_{9/2}$ proton orbital *below* the magic $Z = 50$ shell gap could the trend of the measured $B(E2)$ values be reproduced [1–4]. Recent work [27] indicates that two effects could combine to explain the phenomenon; the inversion of the $d_{5/2}$ and $g_{7/2}$ single-particle levels and the Pauli blocking of neutrons in the $g_{9/2}$ orbital. In contrast, the new data point at ^{108}Te suggests that the reduced transition probabilities for the light tellurium isotopes are not enhanced with respect to the shell model predictions. The present experimental result therefore does not support a “weakening” of the $N, Z = 50$ shell closure as suggested from measurements of $B(E2; 0_{\text{g.s.}}^+ \rightarrow 2^+)$ values for light Sn isotopes [4]. For Te, the two protons above the $Z = 50$ shell gap are an important part of the wave function of the 2_1^+ state, and contribute considerably to the transition probability. We therefore expect that the neutron dependent Pauli blocking effect seen in Sn [27] should be relatively smaller in Te. We also note, see Fig. 3, that the inversion of the $d_{5/2}$, $g_{7/2}$ orbitals in the Te calculation, does not create any substantial effect.

To summarize, we report on a lifetime measurement of the first excited 2^+ state in the extremely neutron deficient nuclide ^{108}Te . The result agrees with the predictions from standard shell model calculations based on the CD-Bonn interaction.

The authors would like to thank the support staff of the Accelerator Laboratory at the University of Jyväskylä for their excellent support, and R. Seppälä for preparing the targets. This work was supported by the Swedish Research Council under Grant Nos. 623-2009-7340, 621-2010-3694, and 2010-4723. It was further supported by the EU 7th framework programme Integrating Activities - Transnational Access, Project No. 262010 (ENSAR) and by the Academy of Finland

under the Finnish Centre of Excellence Programme 2006–2011 (Nuclear and Accelerator Based Physics Programme at JYFL) and Contract No. 131665. We also acknowledge the Nordic Infrastructure support under NordForsk (Project No. 070315). In addition, this work was supported by the

UK Science and Technology Facilities Council and by the JSPS Core-to-Core Program, International Research Network for Exotic Femto System. We finally thank the European GAMMAPOOL network (EUROBALL owners committee) for providing the detectors of JUROGAM II.

-
- [1] A. Banu *et al.*, *Phys. Rev. C* **72**, 061305(R) (2005).
 - [2] J. Cederkäll *et al.*, *Phys. Rev. Lett.* **98**, 172501 (2007).
 - [3] C. Vaman *et al.*, *Phys. Rev. Lett.* **99**, 162501 (2007).
 - [4] A. Ekström *et al.*, *Phys. Rev. Lett.* **101**, 012502 (2008).
 - [5] I. Talmi, *Nucl. Phys. A* **172**, 1 (1971).
 - [6] M. G. Procter *et al.*, *Phys. Lett. B* **704**, 118 (2011).
 - [7] F. Beck, *Prog. Part. Nucl. Phys.* **28**, 443 (1992).
 - [8] C. Beausang and J. Simpson, *J. Phys. G* **22**, 527 (1996).
 - [9] M. Leino *et al.*, *Nucl. Instrum. Methods Phys. Res. B* **99**, 653 (1995).
 - [10] R. Page *et al.*, *Nucl. Instrum. Methods Phys. Res. B* **204**, 634 (2003).
 - [11] R. S. Simon *et al.*, *Zeitschrift für Physik A* **325**, 197 (1986).
 - [12] E. Paul *et al.*, *Phys. Rev. C* **51**, 78 (1995).
 - [13] C. Fransen *et al.*, *J. Phys.: Conf. Ser.* **205**, 012043 (2010).
 - [14] I. Lazarus *et al.*, *IEEE Trans. Nucl. Sci.* **48**, 567 (2001).
 - [15] P. Rahkila, *Nucl. Instrum. Methods Phys. Res. A* **595**, 637 (2008).
 - [16] D. Radford, *Nucl. Instrum. Methods Phys. Res. A* **361**, 297 (1995).
 - [17] A. Dewald *et al.*, *Z. Phys. A* **334**, 163 (1989).
 - [18] F. Seiffert, Program APATHIE, Institut für Kernphysik, Universität zu Köln (1989), unpublished.
 - [19] D. Sohler *et al.*, *Eur. Phys. J. A* **3**, 209 (1998).
 - [20] G. Lane *et al.*, *Phys. Rev. C* **57**, R1022 (1998).
 - [21] I. Darby *et al.*, *Phys. Rev. Lett.* **105**, 162502 (2010).
 - [22] D. Seweryniak *et al.*, *Phys. Rev. Lett.* **99**, 022504 (2007).
 - [23] J. Ressler *et al.*, *Phys. Rev. C* **65**, 044330 (2002).
 - [24] R. Machleidt, *Phys. Rev. C* **63**, 024001 (2001).
 - [25] M. Hjorth-Jensen *et al.*, *Phys. Rep.* **261**, 125 (1995).
 - [26] M. Górska *et al.*, *Phys. Rev. Lett.* **79**, 2415 (1997).
 - [27] T. Bäck *et al.* (to be published).